Surface plasmon resonance in superperiodic metal nanoslits

Haisheng Leong and Junpeng Guo*

Department of Electrical and Computer Engineering, University of Alabama in Huntsville, Huntsville, Alabama 35899, USA
**Corresponding author: guoj@uah.edu*

Received September 2, 2011; revised October 25, 2011; accepted October 31, 2011;
posted November 3, 2011 (Doc. ID 153787); published December 14, 2011

A superperiodic metal nanoslits device is a surface plasmon resonance optical diffraction grating in which each line of the grating consists of an array of finite number metal nanoslits. The metal nanoslits, upon optical excitations, support localized surface plasmon resonance. The superperiod of the nanoslits causes the coherent radiation of the surface plasmon resonance into the far field with angular dispersion. Therefore, localized surface plasmon resonance in the metal nanoslits can be measured with a CCD or a linear photodetector array. In this Letter, we describe a surface plasmon resonance spectral sensor using a superperiodic gold nanoslits array without using an external optical spectrometer.

OCIS codes: 240.6680, 230.1950, 300.6190.

In 1902, R.W. Wood observed dark and bright bands in the diffraction spectrum of a metal reflection grating. The phenomenon could not be explained with the classical diffraction grating theory at that time [1] and was called Wood's anomaly. Now it is understood that Wood's anomaly is due to the excitation of localized surface plasmon resonance in the metallic grating lines upon the optical excitation [2,3]. In the past decade, surface plasmon resonances in metal nanostructures have been investigated intensively due to the progress of nanofabrication technologies. One of the surface plasmon resonance nanostructures is the periodic metal nanoslits array [4–16]. Previously, surface plasmon resonances in metal nanoslits were investigated by using optical spectrometers to measure either the reflection or the transmission from the metal nanoslits. In this paper, we propose and demonstrate a new metal nanoslits structure with which surface plasmon resonances can be measured differently. The new metal nanoslits structure is a superperiodic metal nanoslits array that consists of arrays of finite number gold nanoslits. The finite number of nanoslits arrays are arranged periodically with a large period above the wavelength of surface plasmon resonance of the nanoslits. The large period, called the "superperiod," causes coherent diffractive radiations of localized surface plasmons into the far field when an illuminating light is normally incident onto the nanostructure grating device. The angular dispersion of the optical diffractions projects different spectral components in the surface plasmon resonance to different directions. Therefore, the surface plasmon resonance spectrum in the metal nanoslits can be captured by using a linear detector array or a CCD in one of the diffraction orders without using an external optical spectrometer.

In a superperiodic metal nanoslits array, the metal nanoslits have a small period (p) that is smaller than the wavelength. The small period nanoslits are arranged with a larger period (P) than the wavelength. The larger period, called the "superperiod," can be created by periodically removing nanoslits in a regular nanoslits array. Figure 1 illustrates a superperiodic gold nanoslits device on a quartz substrate. The small period is 420 nm. The superperiod is 2100 nm. The thickness of the gold film is 60 nm. Because the superperiod is above the wavelength of interest, there are high order diffractions. The high order diffractions are angular dispersive. Different spectral components propagate in different directions. Therefore, the CCD photodetector array can capture the spectrum of the first order diffraction.

The transmission and diffractions from the superperiodic nanoslits device can be calculated using the rigorous Fourier mode expansion technique [17–18]. Figure 2 shows the calculated spectra of the zero-order transmission and the first order diffraction from the superperiodic gold nanoslits device upon the normal incidence with the excitation polarization perpendicular to the metal nanoslits. The sharp transmission peak at 0.612 μm wavelength corresponds to the surface plasmon resonance that causes the enhanced zeroth-order transmission (black dash line) in the nanoslits. It shows clearly that the spectral peak wavelength in the first order diffraction spectrum (red line curve) is at the same wavelength of the spectral peak of the zeroth-order transmission. An additional surface plasmon resonance in the device is observed in the zeroth-order transmission and in the first order diffraction at 0.762 μm wavelength. This resonance

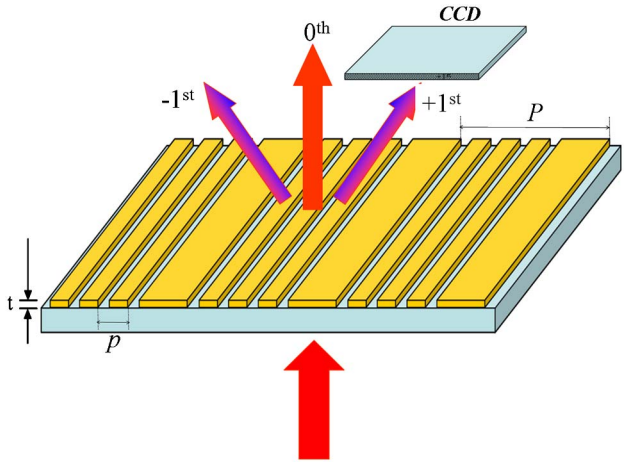

Fig. 1. (Color online) A superperiodic metal nanoslits array with a small period (p) and a large period (P).

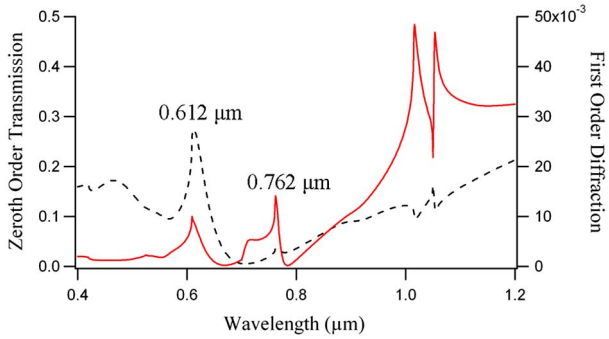

Fig. 2. (Color online) Zeroth-order transmission (black dot curve) and the first order diffraction (red line curve) from a superperiodic nanoslits device.

does not exist in the regular periodic gold nanoslits array. It is due to the surface plasmon resonance in the large period grating made of 700 nm wide gold grating lines.

We fabricate a superperiodic gold nanoslits array with a standard e-beam lithography process. In the fabrication process, we first sputter 2 nm thick chromium adhesion layer and a 60 nm gold film layer on a quartz substrate using the magnetron DC sputtering. Then we spin-coat an about 200 nm electron beam resist (ZEP 520A) layer on top of the gold film. Using the e-beam lithography, we write the nanoslits pattern in the electron beam resist layer and then develop it with the e-beam resist developer (ZED N50). After the e-beam resist pattern has been developed, we use Argon ion gas etching to transfer the e-beam resist pattern to the gold film in a reactive ion etching (RIE) machine. After the Argon ion etching, the e-beam resist is removed. Figure 3 shows the scanning electron microscope (SEM) picture of the fabricated superperiodic nanoslits. The nanoslit's width is 140 nm in the 60 nm thick gold film. The small nanoslit's period is 420 nm. The large period is 2100 nm. The patterned nanoslit's device area is 300 by 300 μm^2.

We test the device with a broadband coherent light source. The broadband light source is a super continuum broadband laser (from NKT photonics, Inc.) with a flat spectrum from 500 nm to 2400 nm wavelength. At the normal incidence from the substrate, the angular dispersion of the first order diffraction is measured with a CCD (Sony ICX098BQ). The polarization of the incident light is perpendicular to the metal nanoslits so that localized surface plasmon resonance can be excited. Figure 4 shows the diffracted and angular dispersed optical signals captured by the CCD imager from the nanoslits device in the air shown in Fig. 4(a), with methanol liquid on the surface Fig. 4(b), and with acetone liquid on the surface Fig. 4(c). The horizontal and vertical numerical numbers represent the pixels on the CCD.

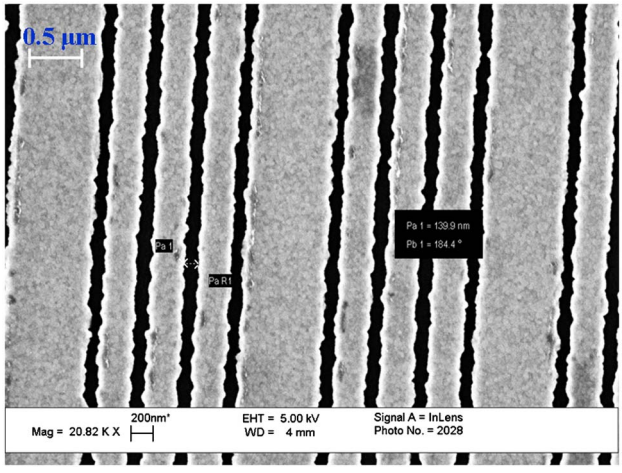

Fig. 3. (Color online) SEM picture of the fabricated superperiodic gold nanoslits array.

In order to obtain the surface plasmon resonance spectrum, we need to find out the correspondence between the wavelengths and the pixels on the CCD. For the first order diffraction at the normal incidence, the diffraction angle is related with the wavelength (λ) and the superperiod (P) as

$$\sin(\theta) = \frac{\lambda}{P}. \tag{1}$$

By measuring the diffraction angle of a known wavelength HeNe laser at 632.8 nm, we can calibrate the measurement setup to find the correspondence between the wavelengths and pixels on the CCD for the first order diffraction. Once the correspondence between the wavelengths and the pixels on the CCD is known, we can plot the surface plasmon resonance measured in the first order diffraction versus the wavelength.

We use methanol and acetone with the refractive index of 1.3284 and 1.3586 to test the integrated surface plasmon sensor. Figure 5(a) shows the zeroth-order transmission spectra from the device in the air (the solid black curve), and when methanol (dotted blue line) and acetone (dotted red line) were applied on the device surface. The acetone was applied later after the measurement for methanol was complete and the methanol was completely vaporized. The zeroth-order transmission spectra in the Fig. 5(a) were measured using a commercial optical spectrometer (Ocean Optics USB 2000). Figure 5(b) shows the first order diffraction spectra measured with our superperiodic nanoslits sensor when the device is in the air (solid black line), methanol solution is applied on the device surface (dotted blue line curve), and acetone solution is applied on the nanoslits surface (dotted red line). The arbitrary unit used for the first order diffraction signal in Fig. 5 corresponds to the intensity levels measured by the CCD. It can be seen that the surface plasmon resonance in the superperiodic nanoslits at

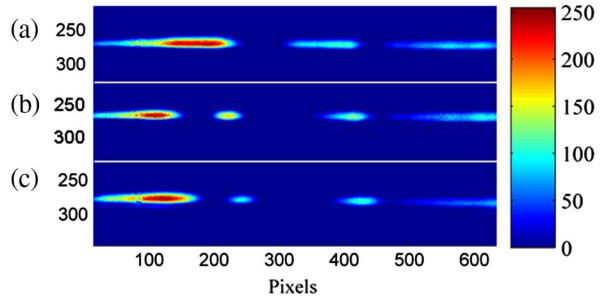

Fig. 4. (Color online) First order diffraction images captured by the CCD when the superperiodic gold nanoslits device is exposed (a) in the air, (b) in the methanol, and (c) in the acetone.

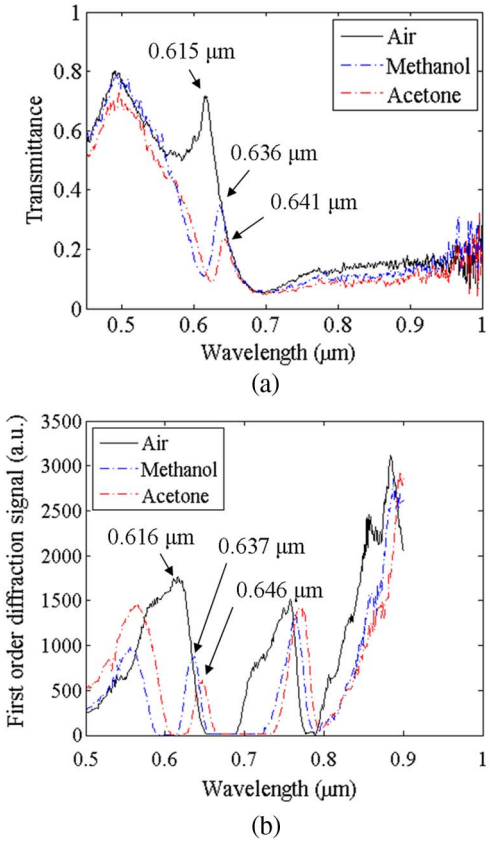

Fig. 5. (Color online) Measured surface plasmon resonance in the superperiodic metal nanoslits device (a) from the zeroth-order transmission and (b) from the first order diffraction.

the wavelength 0.616 μm can be captured by the CCD in the first order diffraction. The resonance wavelength shifts from 0.616 μm in the air to 0.637 μm when methanol is applied, and shifts to 0.646 μm when acetone is applied later. The small difference of resonance wavelengths measured with the external optical spectrometer and our integrated spectral sensor is within the uncertainty range of the external optical spectrometer and our measurement technique. The spectral resolution of the commercial optical spectrometer used in the experiment is 2.0 nm. The spectral resolution of the integrated surface plasmon sensor is 0.7 nm, calculated from the angular dispersion of the superperiodic grating at 0.615 μm wavelength, the pixel size (5.6 μm) on the CCD, and the distance (14.5 mm) between the nanoslits and the CCD.

We calculate the sensitivity of the integrated surface plasmon sensor based on the shift of the resonance wavelength from methanol to acetone. We find that the sensitivity is 298 nm/RIU, which is comparable to the sensitivities of most surface plasmon sensors [19,20]. Significantly, the demonstrated new surface plasmon sensor does not rely on any external optical spectrometers to measure the surface plasmon resonance. The superperiodic metal nanoslits array itself supports localized surface plasmon resonance and performs the spectral analysis simultaneously.

In summary, we have fabricated a superperiod metal nanoslits device and demonstrated a new surface plasmon sensor technique based on the superperiodic metal nanoslits device. The superperiodic nanoslits device has two periods in it. The small period which is subwavelength, provides surface plasmon resonance. The large period provides the diffraction and the angular dispersion of the surface plasmon resonance. The angular dispersion of the diffractions enables the surface plasmon resonance spectra to be measured with a CCD. We have shown through both simulation and experiment that surface plasmon resonance measured in the first order diffraction agrees well with what is measured in the zeroth-order transmission. The new sensor technique integrates the functions of surface plasmon resonance sensing and resonance spectral analysis in a single device, which can be very applicable for making small and integrated chemical and biological sensors.

This work was sponsored by the National Aeronautics and Space Administration (NASA) through the contract NNX07 AL52A and by the National Science Foundation (NSF) through the grant NSF-0814103.

References

1. R. W. Wood, Proc. Phys. Soc. London **18**, 269 (1902).
2. Rayleigh, Phil. Mag. Series 6 **14**, 60 (1907).
3. Y.-Y. Teng and E. A. Stern, Phys. Rev. Lett. **19**, 511 (1967).
4. J. A. Porto, F. J. Garcia-Vidal, and J. B. Pendry, Phys. Rev. Lett. **83**, 2845 (1999).
5. Z. Sun, Y. S. Jung, and H. K. Kim, Appl. Phys. Lett. **86**, 023111 (2005).
6. K. G. Lee and Q. H. Park, Phys. Rev. Lett. **95**, 103902 (2005).
7. P. Lalanne, J. P. Hugonin, and J. C. Rodier, Phys. Rev. Lett. **95**, 263902 (2005).
8. M. Sarrazin, J.-P. Vigneron, and J.-M. Vigoureux, Phys. Rev. B **67**, 085415 (2003).
9. M. M. J. Treacy, Phys. Rev. B **66**, 195105 (2002).
10. Y. S. Jung, J. Wuenschell, H. K. Kim, P. Kaur, and D. H. Waldeck, Opt. Express **17**, 16081 (2009).
11. J. Wuenschell and H. K. Kim, Opt. Express **14**, 10000 (2006).
12. D. Pacifici, H. J. Lezec, H. A. Atwater, and J. Weiner, Phys. Rev. B **77**, 115411 (2008).
13. L. Chen, J. T. Robinson, and M. Lipson, Opt. Express **14**, 12629 (2006).
14. A. Karabchevsky, O. Krasnykov, M. Auslender, B. Hadad, A. Goldner, and I. Abdulhalim, Plasmonics **4**, 281 (2009).
15. K. Lee and P. Wei, Small **6**, 1900 (2010).
16. K. Lee, C. Lee, W. Wang, and P. Wei, J. Biomed. Opt. **12**, 044023 (2007).
17. M. G. Moharam, E. B. Grann, D. A. Pommet, and T. K. Gaylord, J. Opt. Soc. Am. A **12**, 1068 (1995).
18. L. Li, J. Opt. Soc. Am. A **13**, 1024 (1996).
19. A. J. Haes, S. Zou, G. C. Schatz, and R. P. Van Duyne, J. Phys. Chem. B **108**, 109 (2004).
20. M. M. Miller and A. A. Lazarides, J. Phys. Chem. B **109**, 21556 (2005).